

User-customizable Shared Control for Fine Teleoperation via Virtual Reality

Rui Luo^{1*}, Mark Zolotas^{1*}, Drake Moore¹, and Taşkın Padır¹

Abstract—Shared control can ease and enhance a human operator’s ability to teleoperate robots, particularly for intricate tasks demanding fine control over multiple degrees of freedom. However, the arbitration process dictating how much autonomous assistance to administer in shared control can confuse novice operators and impede their understanding of the robot’s behavior. To overcome these adverse side-effects, we propose a novel formulation of shared control that enables operators to tailor the arbitration to their unique capabilities and preferences. Unlike prior approaches to “customizable” shared control where users could indirectly modify the latent parameters of the arbitration function by issuing a feedback command, we instead make these parameters *observable* and *directly* editable via a virtual reality (VR) interface. We present our user-customizable shared control method for a teleoperation task in $SE(3)$, known as the buzz wire game. A user study is conducted with participants teleoperating a robotic arm in VR to complete the game. The experiment spanned two weeks per subject to investigate longitudinal trends. Our findings reveal that users allowed to interactively tune the arbitration parameters across trials generalize well to adaptations in the task, exhibiting improvements in precision and fluency over direct teleoperation and conventional shared control.

I. INTRODUCTION

Teleoperation is the foundation behind many robotic applications. These applications range from preventing human presence in hazardous environments to providing health-care services through remote patient care and robot-assisted surgery. Nevertheless, remotely controlling a complex robot warrants a certain level of operator skill and domain expertise in order to successfully complete challenging teleoperation tasks [1]. Without this baseline, a novice operator may be exposed to detrimental levels of physical and cognitive workload [2], potentially resulting in catastrophic task failures [3]. A common means of relieving this burden on the operator is to employ an autonomous controller that continuously assists the human user by sharing control over the robot [4].

While shared control alleviates excess workload exerted on operators, it may also give rise to new issues that impact task performance and impede dexterity training [5]. One prominent example of such an issue is *model misalignment*. This phenomenon occurs when the division in control between the human and autonomy creates a misunderstanding in how the operator expects the robot to behave [6]. In direct teleoperation, model misalignment may arise whenever a robot

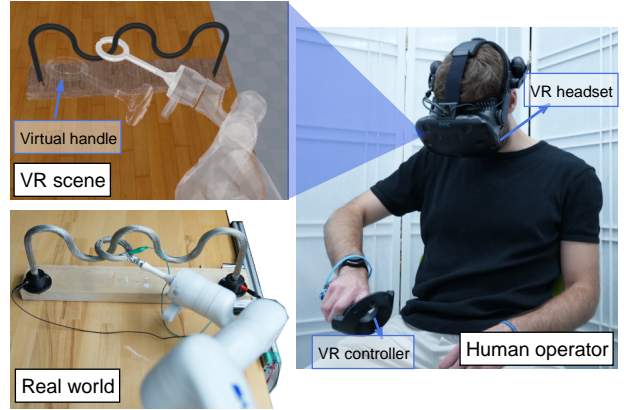


Fig. 1. Illustration of the Kinova Gen 3 robotic arm being teleoperated to play the buzz wire game by a user wearing a virtual reality (VR) headset. The VR controller held by the operator will be represented as a handle in the virtual world, where its simulated effects also have a direct consequence on the physical counterpart played by the robot.

has higher degrees-of-freedom (DoF) than the user’s control interface [7]. Despite this interface asymmetry in DoF, a user with adequate training will still gradually build a mental model of the robot’s behavior. In contrast, the extra layer of arbitration introduced in shared control exacerbates the user’s difficulty in comprehending the system. A communication medium for user feedback is therefore essential to how an operator understands the arbitration [4].

Aside from equipping operators with suitable feedback, another integral aspect of shared control is *user customizability*. Over a long-term interaction, operators will experience variations in their capabilities, preferences, and environments [8]. Shared control must account for these changes and adapt accordingly, especially in terms of how control authority is assigned. Prior works have developed promising frameworks for adaptive shared control by enabling users to either interactively customize the parameters that characterize the arbitration function [9] or suggest corrections for the resulting robot behavior [10], [11]. However, these works rely entirely on the robot’s legible state to convey the effects of a user’s modifications to the arbitration procedure.

In this paper, we establish user-customizable shared control by *directly* communicating the internal parameters of the arbitration function to an operator for refinement. By unveiling these parameters, users can better understand the arbitration process and thus effectively edit its inner workings for personalized outcomes. We ground this idea in a teleoperation task, where operators must remotely control a 7-DoF robotic arm in virtual reality (VR) to complete the

*Equal contributions.

This material is based upon work supported by the National Science Foundation under Award No. 1928654.

¹Institute for Experiential Robotics (IER), Northeastern University, Boston, Massachusetts, USA. {luo.rui, m.zolotas, moore.dr, t.padir}@northeastern.edu

popular buzz wire game (see Fig. 1). The buzz wire game is a suitable testbed due to the need for precise control over both translational and rotational robot motion. This game also requires significant eye-hand coordination and sustained operator focus [12], [13]. Furthermore, the game is frequently utilized for skill training in domains that would benefit from robot teleoperation, such as surgery [14]. To assess the quality and longevity of the proposed shared control method, we conducted a user study that explores patterns in participant performance over repeated interactions.

The key contributions of this paper are as follows:

- A novel mathematical framework that factors in user feedback to formalize user-customizable shared control;
- A comprehensive demonstration of this framework within the context of a teleoperation task in SE(3), involving a real 7-DoF robotic arm and a VR interface as the bidirectional communication channel;
- Results from a longitudinal user study with 12 subjects teleoperating the robotic arm to perform the buzz wire game over four sessions spread across two weeks.

II. RELATED WORK

Sensory feedback can be supplied across multiple modalities in teleoperation. For example, haptic devices are widely used in bilateral teleoperation to simultaneously enhance an operator’s task efficacy and encourage growth in skill [2], [4]. Other modalities, *e.g.*, audio, force, and visual feedback, have enjoyed similar success [15]–[17]. In recent years, VR headsets have proven advantageous in complex manipulation tasks where high-DoF robots are remotely controlled [18]–[20]. Moreover, VR interfaces offer operators the opportunity to modify the inner workings of the teleoperated robot, which is an asset we exploit in this work.

In addition to communication, shared control must also consider arbitration, *i.e.*, how to “blend” a user’s inputs with the autonomous controller’s outputs [4]. An arbitration function is typically described by a set of parameters that determine how control is allocated. These parameters could be fixed, *e.g.*, to primarily favor the human leading, or they could be dynamically updated. In the latter case, a vast bulk of the shared control literature resorts to heuristics for parameter updates, such as safety, fluency, agreement, and confidence [21]–[23]. User-personalized parameters for shared control can also be configured by balancing out the operator’s capability to independently complete a teleoperation task with their need for autonomous assistance [24], [25]. However, the user is unable to configure arbitration parameters in these approaches if no bidirectional communication is available.

Heuristics-based arbitration may be suitable for certain users, but it could also lead to reduced satisfaction or performance in others. To identify the exact form of the “optimal” arbitration function and its corresponding parameters is an intractable problem in real-world teleoperation [9]. Therefore, it may be more appropriate to empower users with the ability to *customize* the arbitration parameters *online*. While previous approaches to customizable shared control

have utilized verbal feedback [9], [26] or corrections [10], [11] to grant this ability, they solely depended on the robot’s observable behavior to explain the control-sharing. Relying on the robot’s appearance and movement to communicate any underlying autonomous assistance is often insufficient [27]. Instead, our paper opts for greater transparency by externalizing the factors that influence arbitration and making them editable to operators.

III. USER-CUSTOMIZABLE SHARED CONTROL

In the following, we propose a mathematical framework for shared control that enables a user to dictate how the robot autonomy should provide teleoperation assistance.

A. Formulation

The shared control system considered in this work is driven by the following interaction data. At time t , a human operator’s measured state, $\mathbf{x}_h(t) \in \mathbb{R}^{n_h}$ (*e.g.*, joystick deflections), is fed into a control interface to produce control commands, $\mathbf{u}_h(t) \in \mathbb{R}^{m_h}$, for direct robot teleoperation. Similarly, a robot’s state and the autonomy’s assistive commands can be denoted as $\mathbf{x}_r(t) \in \mathbb{R}^{n_r}$ (*e.g.*, joint angles, Cartesian poses) and $\mathbf{u}_r(t) \in \mathbb{R}^{m_r}$, respectively.

Under this setup, the output commands of a shared control system adhere to an arbitration process:

$$\mathbf{u}_{sc}(t) = \beta_{\theta}(\mathbf{u}_r(t), \mathbf{u}_h(t)), \quad (1)$$

where $\beta(\cdot)$ is an arbitration function parameterized by time-varying, $\theta(t)$, or time-invariant variables, θ . As an example, the standard linear blending scheme could be written as:

$$\beta_{\theta}(\mathbf{u}_r(t), \mathbf{u}_h(t)) = (1 - \alpha_{\theta})\mathbf{u}_r(t) + \alpha_{\theta}\mathbf{u}_h(t), \quad (2)$$

where $\alpha_{\theta} \in [0, 1]$ is the blending variable and is also a function parameterized by θ [9]. Note that α is frequently treated as a scalar, but in our approach we will adopt a matrix representation to facilitate more granular authority over the system behavior. Let $\mathbf{A}_{\theta} = \text{diag}(\alpha_1, \dots, \alpha_{m_r})$ be a positive definite diagonal arbitration matrix, with $\forall i, \alpha_i \in [0, 1]$, such that the blending scheme is now:

$$\beta_{\theta}(\mathbf{u}_r(t), \mathbf{u}_h(t)) = (\mathbf{I} - \mathbf{A}_{\theta})\mathbf{u}_r(t) + \mathbf{A}_{\theta}\mathbf{u}_h(t), \quad (3)$$

where \mathbf{I} is an identity matrix.

Selecting the parameters, θ , of an arbitration function, $\beta_{\theta}(\cdot)$, is critical in shaping the robot’s assistive behavior. Instead of manually selecting a fixed choice of θ , an “optimal” selection is often derived by solving an optimization problem with an objective function, Γ , such as:

$$\Gamma = \mathcal{L}_T(\mathbf{x}_r(t)) + \sum_{t=0}^{T-1} \mathcal{L}(\mathbf{x}_r(t), \beta_{\theta}(\mathbf{u}_r(t), \mathbf{u}_h(t))), \quad (4)$$

where $\mathcal{L}_T(\cdot)$ is a terminal cost for a horizon, T (*e.g.*, error between the intended and actual target robot states), and $\mathcal{L}(\cdot)$ is an incremental cost (*e.g.*, human effort). Finding a time-invariant θ to minimize Γ will ignore the dynamic nature of the human-robot collaboration. Even if a solution is found with time-varying $\theta(t)$, the core issue remains that Γ might not be the true cost function of the shared control, Γ^* , nor would a tractable solution to Γ^* necessarily exist [9].

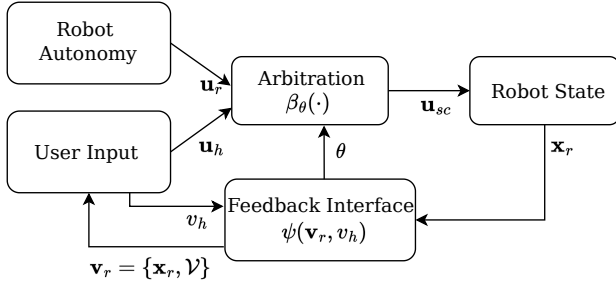


Fig. 2. Diagram of the user-customizable shared control architecture.

B. Feedback-informed User Optimization

To circumvent the intractable problem of identifying Γ^* and its “optimal” parameters, we present a method that allows users to personalize the arbitration function by configuring their preferred θ . The key insight behind our formulation is to establish a bidirectional communication channel between the human and robot. We formalize this channel as a vector-valued function $\psi(\cdot)$ (dropping t for brevity):

$$\theta \leftarrow \psi(\mathbf{v}_r, v_h), \quad (5)$$

where the robot administers feedback, \mathbf{v}_r , to the operator about the shared control, while the user performs parameter updates, $\Delta\theta$, via an interface action, v_h .

For instance, a scalar blending quantity, α , could be derived from the following piece-wise function [9], [25]:

$$\alpha = \begin{cases} 0 & C \leq \theta_1, \\ \frac{\theta_3}{\theta_2 - \theta_1} \cdot C & \theta_1 < C \leq \theta_2, \\ \theta_3 & C > \theta_2, \end{cases} \quad (6)$$

where $\theta_j = \psi_j(\mathbf{v}_r, v_h)$, $j = 1 : K$.

The $\delta\theta_j$ in the K parameter mappings, $\psi_j(\mathbf{v}_r, v_h) = \theta_j \pm \delta\theta_j$, could be obtained from discrete verbal commands made by the operator, $v_h \in \mathbb{Z}^+$ (e.g., “more/less assistance”). Here, the autonomy’s confidence in its estimation of a user’s goal, C , is independent of the resulting arbitration level. We highlight that most previous efforts at user customization of θ_j have solely depended on the robot’s legible state, $\mathbf{v}_r = \mathbf{x}_r$, for operator feedback [9], [26].

In the multi-dimensional arbitration scenario, one could choose to represent \mathbf{A}_θ in a more general form:

$$\mathbf{A}_\theta = \text{diag}(\boldsymbol{\alpha}) = \text{diag}(\alpha_1, \dots, \alpha_{m_r}), \quad (7)$$

$$\text{where } \alpha_i = \sum_{j=1}^K w_j \psi_j(\mathbf{v}_r, v_h), \quad i = 1, \dots, m_r.$$

Each diagonal element, α_i , is governed by potentially more than one factor, θ_j , resultant from $\psi_j(\mathbf{v}_r, v_h)$, as determined by the selection weight, w_j . Whether the arbitration is expressed as Eq. (6) or Eq. (7), the aspiration behind permitting operator customization of θ is to converge on a user-elected optimum, without concretely specifying Γ^* . The overall framework architecture is shown in Fig. 2.

As the feedback variables, \mathbf{v}_r and v_h , dramatically impact how users customize the shared control behavior, we suggest two improvements over prior works in how to produce

these variables. First, the robot’s communication flow should illuminate more than its external state, \mathbf{x}_r . In Section IV, we demonstrate how a set of human-interpretable signals, \mathcal{V} (i.e., visualizations in VR), can be incorporated into $\mathbf{v}_r = \{\mathbf{x}_r, \mathcal{V}\}$ to help operators tune θ . Second, an operator’s parameter updates, $\Delta\theta$, should have a proportionate effect on robot behavior. This proportionality can be achieved by letting the operator submit actions, $v_h \in [0, 1]$ (e.g., using a graphical slider in VR), over the same constrained range as the arbitration parameters, $\forall j, \theta_j \in [0, 1]$.

IV. PROPOSED FRAMEWORK INSTANTIATION

To illustrate the operational principles of the proposed framework, this section provides an instantiation for assistive teleoperation in the scope of the buzz wire game.

A. Testbed: Buzz Wire Game

In the buzz wire game, the operator’s goal is to carefully guide a loop handle in SE(3) from start to end while minimizing collisions with the wire. The game is a well-known assessment environment for fine motor skill and eye-hand coordination [12], [13]. Moreover, 3D buzz wire games are advantageous when evaluating dexterity tasks that benefit from stereoscopic depth perception [12]. As precise motor control, eye-hand coordination, and 3D spatial awareness are critical capabilities for teleoperation in general, we deem this game to be a pertinent testbed. Immersive VR versions of the game have also been validated as an effective simulation for operator training, e.g., in stroke rehabilitation [28], [29]. Hence, we believe a VR setup of the 3D game serves as a suitable experimental arena for our work.

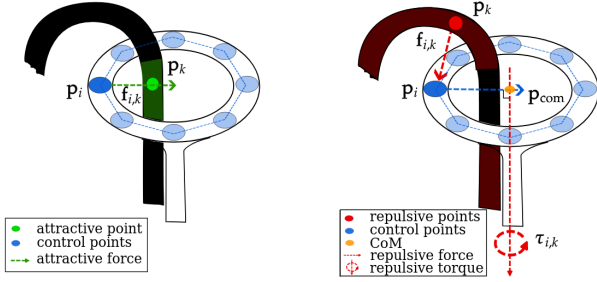
Fig. 1 demonstrates our buzz wire game replica for robot teleoperation. The layout is comprised of a Kinova Gen 3 arm with a loop handle extension at its end-effector to complete the actual game, as well as a person wearing an HTC Vive headset to perform the same task in VR with a handheld controller. A model-based perspective of the buzz wire game and the robot are also constructed in the VR scene. An electric circuit board imitated the game’s “buzz” feature by signaling collisions to the operator in VR. Multimodal feedback cues were triggered upon collision, with red lights flashing and vibrations in the handheld input device.

B. Shared Assistance in Teleoperation

In teleoperation, a common strategy is to control the robot’s end-effector pose, $\mathbf{x}_r \in \mathbb{R}^6$, by sending desired twist commands, $\dot{\mathbf{x}}_d \in \mathbb{R}^6$, via admittance control:

$$\dot{\mathbf{x}}_d = \mathbf{M}^{-1} \int (\mathbf{k} \odot \mathbf{e} + \mathbf{d} \odot \dot{\mathbf{e}} + \mathbf{f}_{\text{ext}}) dt, \quad (8)$$

where $\mathbf{M} \in \mathbb{R}^{6 \times 6}$, $\mathbf{k} \in \mathbb{R}^6$, and $\mathbf{d} \in \mathbb{R}^6$ are the pre-defined mass, stiffness, and damping terms respectively, while $\mathbf{f}_{\text{ext}} \in \mathbb{R}^6$ is the externally applied force, $\mathbf{e} \in \mathbb{R}^6$ is the pose error vector, and \odot denotes component-wise multiplication. In our buzz wire setup, the pose error is the difference between the handheld VR controller’s pose, $\mathbf{x}_h \in \mathbb{R}^6$, and the robot’s state, $\mathbf{x}_r \in \mathbb{R}^6$.



(a) Attractive force $\mathbf{f}_{i,k}$ from attractive point \mathbf{p}_i and environment point \mathbf{p}_k . (b) Repulsive torque $\boldsymbol{\tau}_{i,k}$ from sample collision points on the wire.

Fig. 3. Illustration of how the attractive and repulsive forces are computed given a control point \mathbf{p}_i (dark blue) and environment point \mathbf{p}_k (red).

The robot autonomy can then be integrated into Eq. (8) as an assistive force. By reformulating Eq. (8) as the linear blending scheme shown in Eq. (3), we establish an admittance control policy for shared control as follows:

$$\mathbf{u}_{sc} = \dot{\mathbf{x}}_d = (\mathbf{I} - \mathbf{A}\boldsymbol{\theta})\mathbf{u}_r + \mathbf{A}\boldsymbol{\theta}\mathbf{u}_h, \quad (9)$$

$$\mathbf{u}_h = \mathbf{M}^{-1} \int (\mathbf{k} \odot \mathbf{e} + \mathbf{d} \odot \dot{\mathbf{e}}) dt, \quad (10)$$

$$\mathbf{u}_r = \mathbf{M}^{-1} \int \mathbf{w}_a dt. \quad (11)$$

In this formulation, \mathbf{f}_{ext} has been replaced by a wrench vector, $\mathbf{w}_a \in \mathbb{R}^6$, to represent the autonomous assistance in both translational and rotational space.

C. Real-time Assistive Wrench

Generating real-time autonomous assistance is vital for teleoperation to ensure a reactive user experience and smooth robot motion. To fulfil this requirement, we efficiently compute the assistive wrench, \mathbf{w}_a , using potential fields, where targets produce attractive vectors and obstacles yield repulsive vectors. Attractive and repulsive vectors are typically calculated between a pair of control and environment points [30]. In our setting, we define *eight* control points as the vertices of an octagon that encloses the circular end-effector. The environment points are acquired in real-time given point cloud data detected using two depth cameras.

Environment points within a pre-defined range of the control points compose a neighborhood set, $\mathcal{C} = \mathcal{C}_{att} \sqcup \mathcal{C}_{rep}$, where $|\mathcal{C}| = N$. The \mathcal{C}_{att} subset contains attractive points, whereas \mathcal{C}_{rep} contains repulsive points. The potential forces between an environment point, $\mathbf{p}_k \in \mathcal{C}$, and a control point, $\mathbf{p}_i \in \mathbb{R}^3$, are computed based on a logistic function:

$$\mathbf{f}_{i,k} = \frac{f_{max}}{1 + \exp\left[-\lambda_{i,k} \left(\frac{\|\mathbf{d}\|}{\rho} - d_{i,k}\right)\right]} \hat{\mathbf{d}}_{i,k}, \quad (12)$$

where each function-shaping parameter $\lambda_{i,k} \in \{\lambda_{rep}, \lambda_{att}\}$, $d_{i,k} \in \{d_{rep}, d_{att}\}$, $\hat{\mathbf{d}}_{i,k} = \pm \frac{\mathbf{d}_{i,k}}{\|\mathbf{d}_{i,k}\|}$ has two possible values depending on the relationship between control point i and environment point k (repulsive or attractive). Hence, forces $\mathbf{f}_{i,k}$ can either be repulsive or attractive, with f_{max} determining the maximum magnitude of the generated force and ρ adjusting the change rate in force given distance.

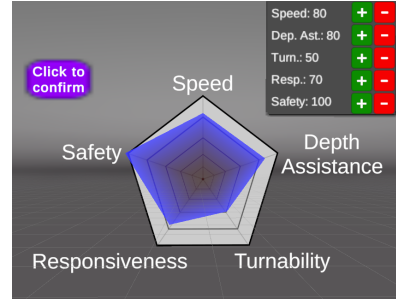


Fig. 4. The customizable spider chart interface in virtual reality. The operator can view and modify assistance across five factors, before confirming their configuration. Each factor is scaled from $[0.1, 1]$ to $[10, 100]$ with a discrete minimal update step of 5.

As the buzz wire game requires 6-DoF teleoperation, we compute the assistive torque $\boldsymbol{\tau}_{i,k}$ for rotational motion as:

$$\boldsymbol{\tau}_{i,k} = \mathbf{f}_{i,k} \times (\mathbf{p}_{com} - \mathbf{p}_i) \quad (13)$$

where \mathbf{p}_{com} is the center of mass of the robot's end-effector. Fig. 3 illustrates an example of how attractive forces and repulsive torques are calculated for the buzz wire game given a pair of control and environment points ($\mathbf{p}_i, \mathbf{p}_k$).

The resultant assistance wrench, $\mathbf{w}_a = [\mathbf{f}_{net}^T \ \boldsymbol{\tau}_{net}^T]^T$, is obtained by aggregating a force component, $\mathbf{f}_{net} \in \mathbb{R}^3$, and a torque component, $\boldsymbol{\tau}_{net} \in \mathbb{R}^3$, each calculated as:

$$\mathbf{f}_{net} = \sum_i \frac{\mathbf{f}_i}{\|\mathbf{f}_i\|} \cdot \max_k \|\mathbf{f}_{i,k}\|, \quad (14)$$

$$\boldsymbol{\tau}_{net} = \sum_i \frac{\boldsymbol{\tau}_i}{\|\boldsymbol{\tau}_i\|} \cdot \max_k \|\boldsymbol{\tau}_{i,k}\|, \quad (15)$$

where $\mathbf{f}_i = \sum_k \mathbf{f}_{i,k}$, $\boldsymbol{\tau}_i = \sum_k \boldsymbol{\tau}_{i,k}$, $i \in \{1, \dots, 8\}$, and $k \in \{1, \dots, N\}$.

D. User-customizable Arbitration

A VR interface acts as the basis for bidirectional communication, $\psi(\mathbf{v}_r, v_h)$, in our user-customizable shared control. We created a spider chart interface, depicted in Fig. 4, to augment the robot's feedback, \mathbf{v}_r , with a variety of human-readable indicators, \mathcal{V} . Specifically, three factors affecting arbitration are displayed in VR: *speed*, *depth assistance*, and *turnability*. *Speed* regulates robot velocity along axes of motion relevant to the buzz wire game (e.g., horizontally along the wire). *Depth assistance* governs the margin between the end-effector and the wire along the depth axis, with the aim of assisting line-of-sight occlusions. *Turnability* adjusts the rotational speed of the end-effector. Users can thus view \mathbf{v}_r , as well as modify the parameters, $\boldsymbol{\theta}$, by supplying edits, v_h , per factor via increment/decrement buttons.

Following the formulation in Eq. (7), the arbitration vector, $\boldsymbol{\alpha} \in \mathbb{R}^6$, is expressed as a linear combination:

$$\boldsymbol{\alpha} = \mathbf{W}\boldsymbol{\theta} = \mathbf{W}\psi(\mathbf{v}_r, v_h) = \mathbf{W} \begin{bmatrix} v_h^{speed} \\ 1 - v_h^{depth} \\ v_h^{turn} \end{bmatrix}, \quad (16)$$

$$\text{where } \mathbf{W} = \begin{bmatrix} 1 & 0 & 1 & 0 & 0.4 & 0.2 \\ 0 & 1 & 0 & 0.2 & 0 & 0 \\ 0 & 0 & 0 & 0.8 & 0.6 & 0.8 \end{bmatrix}^T.$$

The coefficient matrix, $\mathbf{W} \in \mathbb{R}^{6 \times 3}$, is structured in a manner where each editable facet, v_h , directly maps to a θ with a semantically similar effect on arbitration. The weighting of elements was chosen empirically to fit the task. For example, v_h^{turn} is masked by \mathbf{W} to contribute to an 80% change in arbitration on rotation about the z-axis, while v_h^{speed} contributes to the remaining 20%. Here, the term *turnability* intuitively represents more influence over robot rotation than translational speed. The weighting criteria for *depth assistance* uses the complement of v_h^{depth} , as “assistance” implies more contribution from the autonomy.

In addition to task-specific parameters θ , we expose two task-independent parameters: *safety* and *responsiveness*. These parameters adjust f_{max} in Eq. (12) and \mathbf{k} in Eq. (10), respectively, akin to a variable impedance controller. Note that each configurable parameter is actually constrained in the range $[0.1, 1]$ to prevent a “full autonomy” configuration.

V. EXPERIMENT

To gauge the effectiveness of the proposed framework in enhancing teleoperation performance, we conducted a between-subjects study involving 12 subjects (3 female; aged 20-34). Subjects were asked to complete the buzz wire game by teleoperating a robotic arm in VR. All participants provided written consent prior to data collection.

A. Experiment Protocol

Participants were allocated into one of three groups, each designed to evaluate a different control strategy: (1) direct teleoperation (**teleop**), which is implemented by setting $\mathbf{A}_\theta = \mathbf{I}$ in Eq. (9); (2) Shared control with a heuristics-based arbitration function (**sc**), which is described in Section V-B; and (3) our user-customizable shared control method (**sc.user**). Participants were unaware of the distinctions between each group. It is also worth noting that half of the 12 subjects reported no background in robotics. This equal distribution persisted across the control strategies.

Before commencing the experiment, participants in groups **sc** and **sc.user** were provided with identical written explanations of the five arbitration factors, described in Section IV-D. After each trial, these participants could review the updated arbitration factors for the subsequent trial through the VR interface (Fig. 4). Only **sc.user** subjects could edit these factors. All subjects were instructed to complete the game as safely and quickly as possible.

Each group consisted of four participants, and every subject carried out five consecutive trials of the buzz wire game in a single session using their assigned control strategy. This procedure was repeated for a total of four sessions. To evaluate the learning rates of operators over an extended period, a minimum of one workday separated each session, resulting in a two-week duration for the entire experiment. Additionally, the last session involved a distinct wire testbed, as portrayed in Fig. 5. This alteration aimed to assess whether any teleoperation skills gained are transferable to a related, yet different task. Subjects also answered post-session surveys on their user experience.

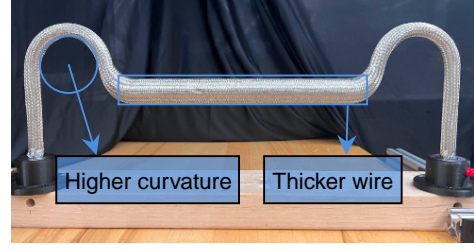


Fig. 5. New wire testbed for the last session to assess skill generalization.

B. Heuristics-based Shared Control

We implemented a heuristics-based assist-as-needed controller as the reference method, **sc**, for our experiments. The arbitration parameters, θ , in this controller are iteratively updated according to the operator’s performance after each trial. We linearly update the parameters with a change rate akin to the multi-trial update function from [24]:

$$\theta_{t+1} = (1 + \chi_t)\theta_t, \quad (17)$$

where t is the trial index and $\chi_t \in \mathbb{R}^3$ is the change rate vector. χ_t is updated using a non-linear function based on the two most recent trials:

$$\chi_t^i = \chi_{\text{nom}} \frac{\bar{r}_t^i - r_d^i}{r_d^i} \left(\frac{|\bar{r}_t^i - r_d^i|}{|\bar{r}_{t-1}^i - r_d^i|} \right)^{\text{sign}(r_d^i - \bar{r}_t^i)}, \quad (18)$$

where r_d^i is the i^{th} component of the desired error vector \mathbf{r}_d , \bar{r}_t^i is the i^{th} component of the average error vector $\bar{\mathbf{r}}_t$ during trial t , and χ_{nom} is the nominal change rate, which determines the maximum change rate within one update step.

Distance from the end-effector to the closest point along the wire is a suitable performance metric to denote safety in the buzz wire game. This error is conveniently contained in the assistive wrench, \mathbf{w}_a , such that $\bar{\mathbf{r}}_t$ can be expressed as:

$$\bar{\mathbf{r}}_t = \mathbf{W}^\dagger \bar{\mathbf{w}}_{a,t}, \quad (19)$$

where $\bar{\mathbf{w}}_{a,t} \in \mathbb{R}^6$ is the average wrench from trial t , \mathbf{W}^\dagger is the pseudo-inverse of the coefficient matrix in Eq. (16), and \mathbf{r}_d is pre-calculated from an expert demonstration.

C. Evaluation Metrics

Performance evaluation for the buzz wire game primarily revolves around two measures: successful task completion time and number of collisions. A trial is deemed successful and collisions are counted when the participant teleoperates the robot’s end-effector to the game end without encountering a fatal failure (when collision forces exceed a threshold). Aside from task time and collisions, we also examine a user’s *jerk* in handling the VR controller (2nd derivative of input velocity commands) to capture “smoothness” [31]. Additionally, we explore the learning trajectories of users, *i.e.*, each user’s change in “skill” metrics relative to their first session. Lastly, we investigate a user’s perceptions of the different control modes in terms of *skill*, *success*, and *difficulty*.

Therefore, the hypotheses for this study are as follows:

- **H1:** Subjects will report higher ratings on skill, success, and difficulty for **sc.user** than **teleop** and **sc**.

TABLE I
SUBJECTIVE RESULTS ACROSS SESSIONS (1 = “VERY LOW” OR “FAILURE”, 10 = “VERY HIGH” OR “PERFECT”)

Sessions	Mode	Skill \uparrow	Success \uparrow	Difficulty \downarrow
1 (baseline)	sc	7.5 \pm 1.0	7.5 \pm 1.3	4.8 \pm 2.2
	sc_user	6.3 \pm 0.5	6.0 \pm 1.8	6.5 \pm 1.7
	teleop	6.8 \pm 1.0	7.5 \pm 1.0	5.5 \pm 2.4
2 & 3 (training)	sc	6.1 \pm 3.9	6.0 \pm 1.6	5.9 \pm 1.8
	sc_user	7.1 \pm 3.8	7.4 \pm 1.4	6.1 \pm 1.4
	teleop	7.6 \pm 3.6	7.5 \pm 1.4	5.8 \pm 2.4
4 (transfer)	sc	6.0 \pm 0.8	6.8 \pm 1.0	5.0 \pm 1.8
	sc_user	7.3 \pm 0.5	7.0 \pm 0.8	5.8 \pm 2.1
	teleop	6.5 \pm 2.4	6.5 \pm 2.4	7.0 \pm 3.6

TABLE II
SUBJECT RESPONSES TO OVERALL EXPERIMENT QUESTIONS (1 = “STRONGLY DISAGREE”, 5 = “STRONGLY AGREE”).

Question	Teleop	SC	SC-User
I found the spider chart <i>helpful</i>	-	3.5 \pm 1.0	4.3 \pm 1.0
Most would learn this robot <i>quickly</i>	4.0 \pm 0.8	3.8 \pm 0.5	4.5 \pm 0.6
The last session was <i>more difficult</i>	3.3 \pm 1.7	2.5 \pm 0.6	3.0 \pm 1.2

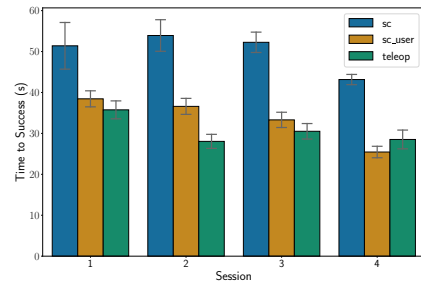
- **H2:** There will be faster task success times and less collisions for **sc_user** than **teleop** and **sc**.
- **H3:** Participants in **sc_user** will exhibit better teleoperation performance relative to their ‘baseline’ session when compared against users from **teleop** and **sc**.

VI. RESULTS

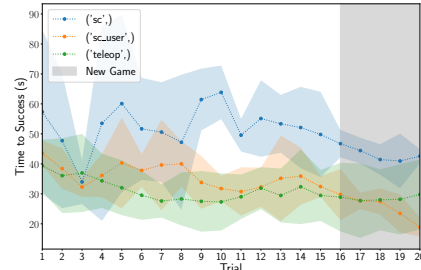
In the following, we report on our results and test our three hypotheses. When evaluating the learning trajectories of participants, we term the first session as the ‘baseline’, the combined second and third sessions as ‘training’, and the last session as ‘transfer’. Unless otherwise stated, mixed ANOVAs were performed to analyze the effects of control modes (between-subjects) and sessions (within-subjects) on the relevant evaluation metrics. The ‘baseline’ session was left out of the ANOVAs, leaving only the combined ‘training’ sessions to compare against the ‘transfer’ condition.

A. Subjective Results

Subject ratings to post-session questions on *skill* (“How would you rate your skill?”), *success* (“How successful were you?”), and *difficulty* (“How hard did you have to work?”) are shown in Table I. For the ‘baseline’ session, **sc** subjects self-reported better ratings than the other two groups, especially in terms of perceived difficulty, with a mean difference of 1.7 between **sc** and **sc_user**. There is a tendency toward more favorable responses for **teleop** and **sc_user** in the ‘training’ sessions, with **teleop** receiving the best ratings across all categories. Nevertheless, **sc_user** has the superior ‘transfer’ according to perceived skill (7.3 \pm 0.5) and success (7.0 \pm 0.8). The **teleop** users found the new wire testbed most difficult to complete (7.0 \pm 3.6), with a mean score difference of 2.0 from **sc** and 1.2 from **sc_user**. Despite these patterns, no main or interaction effects were revealed from the mixed ANOVAs performed on each question category. Based on these tests, we cannot substantiate **H1**.



(a) Time-to-success per session



(b) Time-to-success per trial

Fig. 6. Time-to-success demonstrated for participants across (a) sessions and (b) trials. Gray shaded area represents the session with a new test bed.

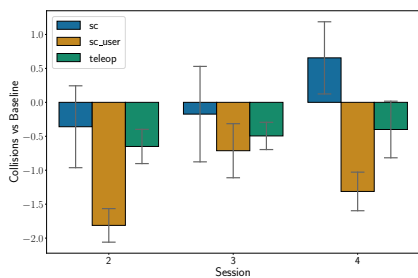
TABLE III
QUANTITATIVE RESULTS ACROSS SESSIONS

Sessions	Mode	Collisions	Time (s)	No. Fails
1 (baseline)	sc	1.74 \pm 2.6	51.4 \pm 24.8	1
	sc_user	2.74 \pm 1.9	38.4 \pm 8.5	1
	teleop	2.10 \pm 1.8	35.8 \pm 9.8	0
2 & 3 (training)	sc	1.60 \pm 2.0	53.1 \pm 12.8	6
	sc_user	1.50 \pm 1.3	35.0 \pm 8.5	0
	teleop	1.54 \pm 1.4	29.3 \pm 8.0	1
4 (transfer)	sc	2.26 \pm 1.9	43.2 \pm 5.4	1
	sc_user	1.45 \pm 1.1	25.5 \pm 6.3	0
	teleop	1.70 \pm 1.4	28.5 \pm 10.3	0

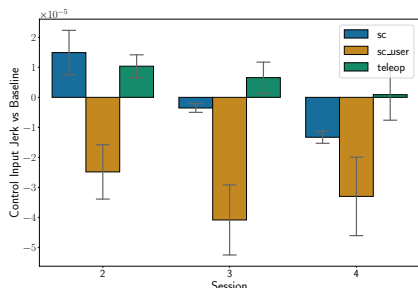
Survey questions on the entire experiment are summarized in Table II. Indeed, the last session is voted as marginally more difficult by **teleop** participants. Subjects in the **sc_user** group also viewed operating the robot as “quicker” to grasp than the other modes. Interestingly, **sc_user** participants considered the spider chart to be more “helpful” (4.3 \pm 1.0) than the **sc** chart (3.5 \pm 1.0), which had autonomously computed values and could not be edited. All **sc_user** individuals “found the VR interface easy to edit” (5.0, not in table).

B. Quantitative Results

Table III summarizes the quantitative results of the study. In the first ‘baseline’ session, the **sc** group had the least number of collisions (1.74 \pm 2.6), whereas **teleop** had the fastest time-to-success (35.8s \pm 9.8s). On the other hand, **sc_user** subjects exhibited notable progress in ‘training’ sessions, as there was a major reduction in average number of collisions, yielding the lowest collision count (1.50 \pm 1.3). The **teleop** group continued to maintain the fastest success times (29.3s \pm 8.0s). Although in the ‘transfer’ session, **sc_user** participants attained the swiftest completion times



(a) Collisions vs baseline per session



(b) Control interface jerk vs baseline per session

Fig. 7. Differences in collision occurrences (a) and control interface jerk (b) relative to the subject’s average baseline performance in the first session.

(25.5s \pm 6.3s) and the fewest collisions (1.45 \pm 1.1).

Average time-to-success is presented per session and trial in Figs. 6(a) and 6(b), respectively. A mixed ANOVA run on completion times found no interaction effect between modes and sessions ($F(2, 9) = 1.17, p = 0.35$). Though a main effect was found for both mode ($p < 0.01$) and session ($p < 0.05$). Post-hoc pairwise comparisons validated that the **sc** times were slower than those for both **teleop** ($p < 0.01$) and **sc_user** ($p < 0.001$). A paired post-hoc test also suggests that completion times were faster in the final session ($p < 0.05$), hinting at the ‘transfer’ task being a quicker game to navigate. These results only partially support **H2**, as **teleop** and **sc_user** obtained statistically similar times ($p = 0.81$). Nevertheless, we highlight the trend in **sc_user** operators displaying faster task times compared to the **teleop** group when transitioning to the new testbed. Smaller standard deviations also bolster this trend, as shown in Fig. 6(b).

Comparing a subject’s teleoperation performance between their ‘baseline’ session and subsequent sessions is informative of their learning trajectory. Figs. 7(a) and 7(b) illustrate these trajectories for collision frequency and controller jerk, respectively, which we use to quantify operator ‘skill’. A mixed ANOVA for collisions found no interaction or main effects in modes and session. Yet a one-way ANOVA to observe if the control mode in the ‘transfer’ session influenced collisions relative to the subject’s ‘baseline’ revealed a significant effect ($F(2, 56) = 5.47, p < 0.01$). Post-hoc comparisons showed that the only significant effect was **sc_user** incurring fewer relative collisions than **sc** ($p < 0.01$). Similarly, a mixed ANOVA found no interactions or main differences on control interface jerk, but a one-way ANOVA found a significant effect of mode in the final session ($F(2, 57) = 3.52, p < 0.05$). A post-hoc test indicated that

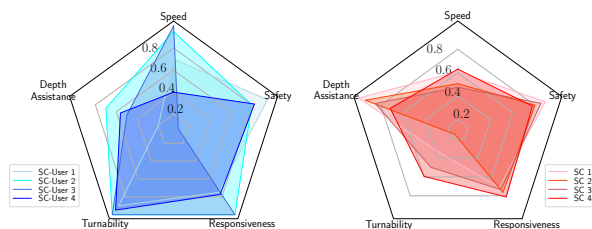


Fig. 8. User-customized vs heuristics-based arbitration parameters at the conclusion of the experiment.

sc_user issued less jerky commands than **teleop** ($p < 0.05$). Overall, these findings offer partial support for **H3**.

VII. DISCUSSION

A few notable findings emerged from the buzz wire experiment. First, while the subjective and *absolute* quantitative results were comparable for **sc_user** and **teleop** during ‘training’ sessions, **sc_user** operators outperformed the other two control modes in measures of *relative* improvement. For example, **sc_user** subjects had consistently less collisions and produced less jerky control inputs than their ‘baseline’ session, which were statistically significant differences over **teleop** and **sc** in the ‘transfer’ condition. Indeed, **sc_user** obtained markedly better results across all subjective and quantitative (absolute and relative) metrics in the new game. Altogether, these results reinforce the benefits of offering users an intuitive means of customizing shared control, particularly when there are variations in the task.

Another key observation is the inferior performance of the **sc** policy. Comparing the distributions of arbitration parameters between **sc_user** and **sc** reveals higher variance in the **sc_user** group’s final selection of θ , as depicted in Fig. 8. The invariance in **sc** is due to the performance heuristic \bar{r}_t from Eq. (19) being solely dependent on the distance between the end-effector and wire. An alternative update routine based on \bar{r}_t could prioritize factors that **sc_user** participants gravitated toward, such as *turnability* and *responsiveness*. However, any heuristics-based method for automatically adapting θ would still converge to a similar parameter distribution across users, without accounting for individual preferences. Shared control policies learnt from large demonstration datasets, *e.g.*, using reinforcement learning [32], would also suffer from the lack of personalization to unseen users. Moreover, labeling arbitration parameters for a dataset requires regular human intervention and is thus difficult to simulate or acquire.

Lastly, we believe our formulation for user-customizable shared control can be applied to a broad range of teleoperation contexts. This formulation not only modeled arbitration factors that are specific to the task (*depth assistance*, *speed*, and *turnability*), but also incorporated task-independent factors, such as *safety* to tune the potential force magnitude and *responsiveness* to adjust the stiffness in admittance control. One could also extend the proposed shared control formulation to treat the dimensions of latent actions learnt from expert demonstrations as user-adjustable [11], [32], [33]. The main challenge here would be in communicating these

dimensions through \mathcal{V} , and supplying interface actions, v_h , to modify their values. Each independent latent dimension may not represent an interpretable factor of variation, nor occupy a constrained space of values for easy editing via v_h . We defer investigation into this idea for future work.

VIII. CONCLUSIONS

In this paper, we introduced a mathematical shared control framework for users to customize the arbitration process. We presented an instantiation of this framework for a teleoperation task in SE(3) and conducted a longitudinal study spanning two weeks per subject to evaluate the proposed method. Our user-customizable shared control method enhanced teleoperation outcomes, including collision frequency and input jerk, while also accommodating the baseline skill levels of different users. Furthermore, operators transferred to generalizations in the teleoperation task better when they could edit the inner workings of the shared control. We believe these preliminary results hold promise for long-term adaptability to diverse variations in users and tasks. Future research directions will increase the participant sample size, explore a wider array of teleoperation tasks, and consider more flexible representations of the arbitration parameters for communication and user editing.

REFERENCES

- [1] K. Darvish, L. Penco, J. Ramos, R. Cisneros, J. Pratt, E. Yoshida, S. Ivaldi, and D. Pucci, "Teleoperation of humanoid robots: A survey," *IEEE Transactions on Robotics*, 2023.
- [2] M. Selvaggio, M. Cognetti, S. Nikolaidis, S. Ivaldi, and B. Siciliano, "Autonomy in physical human-robot interaction: A brief survey," *IEEE Robotics and Automation Letters*, vol. 6, no. 4, pp. 7989–7996, 2021.
- [3] R. Luo, C. Wang, C. Keil, D. Nguyen, H. Mayne, S. Alt, E. Schwarm, E. Mendoza, T. Padir, and J. P. Whitney, "Team Northeastern's Approach to ANA XPRIZE Avatar Final Testing: A Holistic Approach to Telepresence and Lessons Learned," in *IEEE/RSJ International Conference on Intelligent Robots and Systems*, 2023, pp. 7054–7060.
- [4] D. P. Losey, C. G. McDonald, E. Battaglia, and M. K. O'Malley, "A Review of Intent Detection, Arbitration, and Communication Aspects of Shared Control for Physical Human–Robot Interaction," *Applied Mechanics Reviews*, vol. 70, no. 1, 2018.
- [5] M. K. O'Malley, A. Gupta, M. Gen, and Y. Li, "Shared Control in Haptic Systems for Performance Enhancement and Training," *Journal of Dynamic Systems, Measurement, and Control*, vol. 128, no. 1, pp. 75–85, 2005.
- [6] M. Zolotas and Y. Demiris, "Towards Explainable Shared Control using Augmented Reality," in *IEEE/RSJ International Conference on Intelligent Robots and Systems*, 2019, pp. 3020–3026.
- [7] S. Musić and S. Hirche, "Control sharing in human-robot team interaction," *Annual Reviews in Control*, vol. 44, pp. 342–354, 2017.
- [8] B. D. Argall, "Autonomy in rehabilitation robotics: An intersection," *Annual Review of Control, Robotics, and Autonomous Systems*, vol. 1, no. 1, pp. 441–463, 2018.
- [9] D. Gopinath, S. Jain, and B. D. Argall, "Human-in-the-loop optimization of shared autonomy in assistive robotics," *IEEE Robotics and Automation Letters*, vol. 2, no. 1, pp. 247–254, 2017.
- [10] M. Hagenow, E. Senft, R. Radwin, M. Gleicher, B. Mutlu, and M. Zinn, "Corrective Shared Autonomy for Addressing Task Variability," *IEEE Robotics and Automation Letters*, vol. 6, no. 2, pp. 3720–3727, 2021.
- [11] Y. Cui, S. Karamcheti, R. Palleti, N. Shivakumar, P. Liang, and D. Sadigh, "No, to the right: Online language corrections for robotic manipulation via shared autonomy," in *ACM/IEEE International Conference on Human-Robot Interaction*, 2023, pp. 93–101.
- [12] J. C. A. Read, S. F. Begum, A. McDonald, and J. Trowbridge, "The Binocular Advantage in Visuomotor Tasks Involving Tools," *i-Perception*, vol. 4, no. 2, pp. 101–110, 2013.
- [13] F. Budini, M. M. Lowery, M. Hutchinson, D. Bradley, L. Conroy, and G. De Vito, "Dexterity training improves manual precision in patients affected by essential tremor," *Archives of Physical Medicine and Rehabilitation*, vol. 95, no. 4, pp. 705–710, 2014.
- [14] H. Schreuder, C. van den Berg, E. Hazebroek, R. Verheijen, and M. Schijven, "Laparoscopic skills training using inexpensive box trainers: which exercises to choose when constructing a validated training course," *BJOG: An International Journal of Obstetrics & Gynaecology*, vol. 118, no. 13, pp. 1576–1584, 2011.
- [15] M. J. A. Zeestraten, I. Havoutis, and S. Calinon, "Programming by demonstration for shared control with an application in teleoperation," *IEEE Robotics and Automation Letters*, vol. 3, no. 3, pp. 1848–1855, 2018.
- [16] D. Nicolis, *A General Framework for Shared Control in Robot Teleoperation with Force and Visual Feedback*. Springer International Publishing, 2020, pp. 119–131.
- [17] K. Fitzsimons, A. Kalinowska, J. P. Dewald, and T. D. Murphey, "Task-based hybrid shared control for training through forceful interaction," *The International Journal of Robotics Research*, vol. 39, no. 9, pp. 1138–1154, 2020.
- [18] R. Hetrick, N. Amerson, B. Kim, E. Rosen, E. J. d. Visser, and E. Phillips, "Comparing Virtual Reality Interfaces for the Teleoperation of Robots," in *Systems and Information Engineering Design Symposium*, 2020, pp. 1–7.
- [19] M. Zolotas, M. Wonsick, P. Long, and T. Padir, "Motion Polytopes in Virtual Reality for Shared Control in Remote Manipulation Applications," *Frontiers in Robotics and AI*, vol. 8, p. 286, 2021.
- [20] E. Babaian, D. Yang, M. Karimi, X. Xu, S. Ayvasik, and E. Steinbach, "Skill-cpd: Real-time skill refinement for shared autonomy in manipulator teleoperation," in *IEEE/RSJ International Conference on Intelligent Robots and Systems*, 2022, pp. 6189–6196.
- [21] Q. Li, W. Chen, and J. Wang, "Dynamic shared control for human-wheelchair cooperation," in *IEEE International Conference on Robotics and Automation*, 2011, pp. 4278–4283.
- [22] A. D. Dragan and S. S. Srinivasa, "A policy-blending formalism for shared control," *The International Journal of Robotics Research*, vol. 32, no. 7, pp. 790–805, 2013.
- [23] M. Zurek, A. Bobu, D. S. Brown, and A. D. Dragan, "Situational confidence assistance for lifelong shared autonomy," in *IEEE International Conference on Robotics and Automation*, 2021, pp. 2783–2789.
- [24] A. U. Pehlivan, D. P. Losey, and M. K. O'Malley, "Minimal assist-as-needed controller for upper limb robotic rehabilitation," *IEEE Transactions on Robotics*, vol. 32, no. 1, pp. 113–124, 2016.
- [25] S. Jain and B. Argall, "Probabilistic Human Intent Recognition for Shared Autonomy in Assistive Robotics," *ACM Transactions on Human-Robot Interaction*, vol. 9, no. 1, 2019.
- [26] C. X. Miller, T. Gebrekristos, M. Young, E. Montague, and B. Argall, "An analysis of human-robot information streams to inform dynamic autonomy allocation," in *IEEE/RSJ International Conference on Intelligent Robots and Systems*, 2021, pp. 1872–1878.
- [27] C. Brooks and D. Szafrir, "Visualization of intended assistance for acceptance of shared control," in *IEEE/RSJ International Conference on Intelligent Robots and Systems*, 2020, pp. 11425–11430.
- [28] C. G. Christou, D. Michael-Grigoriou, and D. Sokratous, "Virtual Buzzwire: Assessment of a Prototype VR Game for Stroke Rehabilitation," in *IEEE Conference on Virtual Reality and 3D User Interfaces*, 2018, pp. 531–532.
- [29] U. Radhakrishnan, L. Kuang, K. Koumaditis, F. Chinello, and C. Pacciarotti, "Haptic feedback, performance and arousal: A comparison study in an immersive vr motor skill training task," *IEEE Transactions on Haptics*, pp. 1–13, 2023.
- [30] F. Flacco, T. Kröger, A. De Luca, and O. Khatib, "A depth space approach to human-robot collision avoidance," in *IEEE international conference on robotics and automation*, 2012, pp. 338–345.
- [31] N. Hogan and D. Sternad, "Sensitivity of smoothness measures to movement duration, amplitude, and arrests," *Journal of Motor Behavior*, vol. 41, no. 6, pp. 529–534, 2009.
- [32] S. Reddy, A. Dragan, and S. Levine, "Shared autonomy via deep reinforcement learning," in *Proceedings of Robotics: Science and Systems*, 2018.
- [33] H. J. Jeon, D. Losey, and D. Sadigh, "Shared autonomy with learned latent actions," in *Robotics: Science and Systems*, 2020.